Statistical Analyses of Adhesive Forces on Electrophotographic Toners

Inan Chen
Quality Engineering Associates, Inc.
755 Middlesex Turnpike, Unit 3, Billerica MA 01821
Tel: 978-528-2034 · Fax: 978-528-2033
e-mail: info@qea.com
URL: www.qea.com

Paper presented at the IS&T's NIP19
International Conference on Digital Printing Technologies
September 28–October 3, 2003, New Orleans, Louisiana

Statistical Analyses of Adhesive Forces on Electrophotographic Toners

Inan Chen
Quality Engineering Associates (QEA), Inc., Burlington, Massachusetts

Abstract

The statistical distributions of toner adhesive force F_a and detach field E_d, arising from distributions in toner radius r and charge density q are examined mathematically. The widening of F_a distribution and the narrowing of E_d distribution, compared to r and/or q distributions, have been predicted. Since E_d is a quantity more relevant than F_a in electrophotography, this finding suggests that the effects of toner size and/or charge dispersions on toner adhesion in electrophotography may be weaker than generally expected.

Introduction

Adhesion of toner particles to a surface is a phenomenon important in many sub-processes of electrophotography, e.g., development, transfer and cleaning. Extensive studies over the last 30+ years have addressed various features of particle-surface adhesion.[1] While much progress has been made, confusing experimental results have also been reported. This is often attributed to the size, shape and/or charge variations among the particles within a sample in practical applications. Investigations on samples with mono-dispersed spherical particles have been carried out to avoid this problem. However, understanding the nature of poly-dispersed samples is indispensable for advancement of the technology. In this work, we investigate the statistical consequences of toner size and charge dispersions on the adhesion and detachment processes.

Recently, an investigation of toner adhesion using a novel apparatus based on vibratory detachment of toners was reported by Hirayama et al.[2] The toner size and charge dependences of the adhesive force were determined for samples with poly-dispersed size, shape and charge. The empirical relationship obtained is consistent with the expression derived by Rimai et al. from the theory of Johnson et al.[1,3] Based on these works, the adhesive force, F_a, can be expressed as the sum of an electrostatic component F_{es} and a non-electrostatic component F_{ne} as,

$$F_a(r, q) = F_{es} + F_{ne} = 4\pi(A_{es}r^2q^2 + A_{ne}r) \quad (1)$$

where r is the toner radius, q is the area density of charge on toners, and A_{es} and A_{ne} are two empirically determined constants.

In most electrophotographic sub-processes, toners are removed from a surface with an electrostatic force, i.e. the product of toner charge and the external field. Denoting the charge on a toner by $Q = 4\pi r^2 q$, the required detach field E_d is given by,

$$E_d(r, q) = F_a/Q = A_{es}q + A_{ne}/rq \quad (2)$$

For typical electrophotographic toners on polished titanium surface, the values found for the constants are,[2]

$$A_{es} \approx 1.63\text{x}10^{11}\ \text{Nm}^2/\text{C}^2, A_{ne} \approx 6.34\text{x}10^{-4}\ \text{N/m} \quad (3)$$

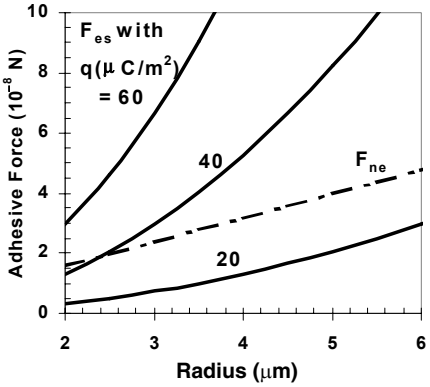

Figure 1. Electrostatic F_{es} (solid) and non-electrostatic F_{ne} (dashed) components of adhesive force F_a vs. toner radius

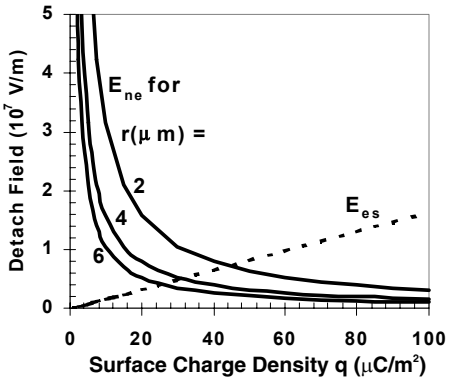

Figure 2. Electrostatic E_{es} (dashed) and non-electrostatic E_{ne} (solid) components of detach field E_d vs. toner surface charge density

With these constant values, the size and charge density dependences of the two components, F_{es} and F_{ne} are shown in Fig. 1 for r and q in the ranges of practical interest. It can be seen that at higher charge densities F_{es} is larger than F_{ne}, while at lower charge densities the relation is reversed. The transition occurs at about $q \approx 40\ \mu C/m^2$. Similar plot of the two components of the detach field E_d is shown in Fig. 2. As in the case of F_a (Fig.1), the dominance of non-electrostatic or electrostatic components changes at charge density value $q \approx 40\ \mu C/m^2$. For a toner radius of 4 μm, this q value corresponds to a charge-to-mass ratio of $Q/m \approx 30\ \mu C/g$, which is in the range of typical Q/m values for toner samples in actual electrophotographic applications.

Because of the wide distributed values of radius r and charge density q in toner samples, the adhesive force F_a and the detach field E_d for individual toners, as related to r and q by Eqs.(1) and (2), respectively, can be expected to have widely distributed values. The objective of the present work is to investigate the statistical consequences of r and q distributions on the F_a and E_d distributions.

Log-Normal Distributions

It is well known that the toner size distribution can be described by a log-normal distribution. The charge density distribution is less well documented, but can also be assumed to be log-normal with little loss of generality.

The probability distribution function (PDF) of a random variable x (e.g., r and q) with the log-normal distribution is given by,[4,5]

$$p(x) = [1/\sqrt{(2\pi)}\alpha x]\exp\{-[ln(x/\xi)/\alpha]^2/2\} \quad (4)$$

and the cumulative probability function (CPF) by,

$$P(x) = \int_0^x p(x')dx' = \{1 + \mathrm{erf}[ln(x/\xi)/(\sqrt{2})\alpha]\}/2 \quad (5)$$

where erf is the error function, and $\xi = x_{md}$ is the median value, i.e., $P(\xi) = 0.5$. The relative standard deviation (RSD) δ, i.e., the ratio of standard deviation σ to the average x_o, is related to the parameter α by,

$$\mathrm{RSD}: \delta = \sigma/x_o = [\exp(\alpha^2) - 1]^{1/2} \quad (6)$$

where $\sigma = [\langle x^2\rangle - x_o^2]^{1/2}$, with $\langle x^2\rangle$ denoting the average of x^2.

Another measure of the width of distribution, the geometric standard deviation (GSD) is defined in terms of two x values, $x_1 = \xi\exp(-\alpha)$ and $x_2 = \xi\exp(\alpha)$, with $P(x_1) = 0.16$ and $P(x_2) = 0.84$ as,

$$\mathrm{GSD} = \xi/x_1 = x_2/\xi = (x_2/x_1)^{1/2} = \exp(\alpha) \quad (7)$$

In other words, GSD represents the half width, in logarithmic scale, of the central 68% of the distribution.

Adhesive Force and Detach Field Distributions

The experimental data on the distribution of adhesive forces F_a reported by Hirayama et al.[6] can be replotted as a CPF vs. F_a shown as solid curve with data points in Fig. 3. From the F_a value corresponding to the CPF value P = 0.5, the median adhesion is found to be $F_m = 0.8\times10^{-7}$ N. Similarly, from $P(F_1) = 0.16$ and $P(F_2) = 0.84$, we find $F_1 = 0.36\times10^{-7}$ N and $F_2 = 1.32\times10^{-7}$ N, yielding the GSD of F_a as $GSD(F_a) = (F_2/F_1)^{1/2} = 1.91$, or $\alpha = 0.65$ from Eq.(7). The dashed curve in Fig. 3 is the CPF of a log-normal distribution, Eq.(5), calculated with these median F_m and α (or GSD) values. It can be seen that the measured F_a distribution is approximately log-normal.

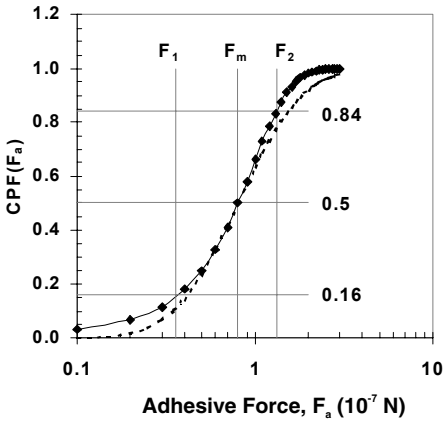

Figure 3. CPF of adhesive force from ref. 6 (solid-data), and the fitted log-normal CPF (dashed)

In the following, we shall examine the nature of adhesive force and detach field distributions, derived from the toner radius r and the charge density q distributions, based on the functional relationship, Eqs.(1) and (2), suggested experimentally and theoretically.[1,2]

The average value $\langle Y(r, q)\rangle$ of a function Y of r and q, both of which have log-normal distributions, can be calculated by,

$$\langle Y(r, q)\rangle = \int_0^\infty [\int_0^\infty Y(r, q)p(r)dr]p(q)dq \quad (8)$$

where p(r) and p(q) are the log-normal PDF, Eq.(4), for r and q respectively. The integral can easily be evaluated by using the formula for the average $\langle x^n\rangle$ of n-th power of x, x^n, (x = r or q), given by,

$$\langle x^n\rangle = \int_0^\infty x^n p(x)dx = x_o^n g_x^{n(n-1)/2} \quad (9)$$

with g_x defined in terms of the RSD of x distribution δ_x as $g_x = 1+\delta_x^2$. Applying this general formula to the non-electrostatic and electrostatic components of F_a and E_d, we have from Eqs.(1) and (2),

$$\langle F_{ne}\rangle = 4\pi A_{ne}\langle r\rangle = 4\pi A_{ne} r_o \quad (10a)$$

$$\langle F_{es}\rangle = 4\pi A_{es}\langle r^2\rangle\langle q^2\rangle = 4\pi A_{es} r_o^2 q_o^2 g_r g_q \quad (10b)$$

$$\langle E_{ne}\rangle = A_{ne}\langle r^{-1}\rangle\langle q^{-1}\rangle = (A_{ne}/r_o q_o) g_r g_q \quad (11a)$$

$$\langle E_{es}\rangle = A_{es}\langle q\rangle = A_{es} q_o \quad (11b)$$

It can be seen that while the average value of F_{ne} depends on the average r_o only, the average value of F_{es} is a function of, not only the averages but also the widths of the r and q distributions. Consequently, it has a larger value than that calculated at the averages r_o and q_o. For E_d, this situation is reversed, namely, the average $\langle E_{ne}\rangle$ is dependent on the widths of r and q distributions, but the average $\langle E_{es}\rangle$ is not, as seen from Eqs.(11a,b). Such a unique dependency on the distribution widths (g or δ) should be taken into consideration when comparing the relative sizes of the non-electrostatic and the electrostatic components.

In the special case that only the radius has distributed values, but the charge density has a definite value q, the F_a and E_d distributions can be evaluated from the log-normal PDF (or CPF) of r distribution. Figure 4 shows a set of PDF's with the median r_m = 4 μm, the RSD δ_r = 0.8 and a fixed q = 40μC/m^2. The PDF(r) curve is a plot of p(r), calculated from Eq.(4), against the r values. The PDF(F_a) and PDF(E_d) curves are obtained by plotting the p(r) values against the F_a(r) and E_d(r) values calculated from Eqs. (1) and (2), respectively. Similar procedures using the CPF P(r), Eq.(5), instead of p(r), yields the CPF(r), CPF(F_a) and CPF(E_d) shown in Fig. 5.

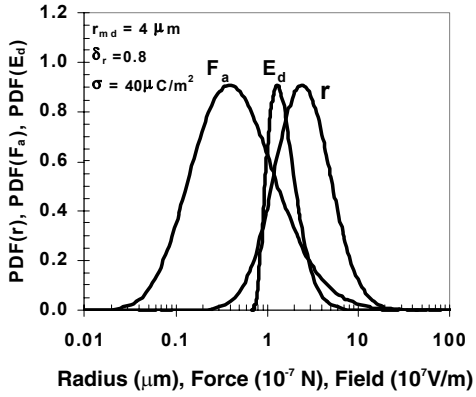

Figure 4. PDF of adhesive force F_a and detach field E_d, due to a given radius distribution PDF(r)

An important feature seen from the curves in Figs. 4 and 5 is the widening of the F_a distribution and the narrowing of E_d distribution compared to the r distribution. This indicates that the effect of toner size dispersion on E_d, a quantity more important than F_a in electrophotography, is much weaker than the same effect on F_a, a quantity often measured in adhesion experiments. In the following, we shall show that this feature is generally expected even with distributed charge density q.

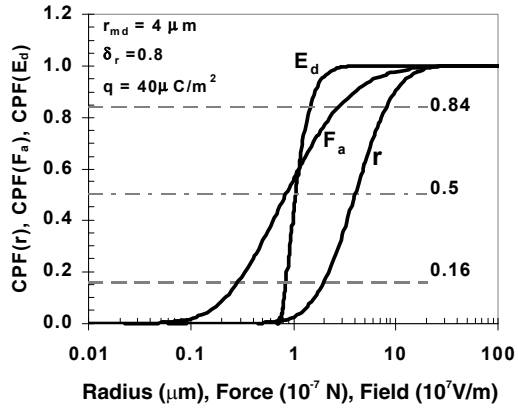

Figure 5. CPF of adhesive force F_a and detach field E_d, due to a given radius distribution CPF(r)

The RSD of F_a can be calculated from the averages of F_a and F_a^2 as,

$$\begin{aligned} RSD(F_a) &= [\langle F_a^2\rangle - \langle F_a\rangle^2]^{1/2}/\langle F_a\rangle \\ &= [A_{ne}^2(g_r - 1) + 2A_{ne}A_{es} r_o q_o g_r g_q (g_r^2 - 1) \\ &\quad + A_{es}^2 r_o^2 q_o^4 g_r^2 g_q^2 (g_r^4 g_q^4 - 1)]^{1/2}/(A_{ne} + A_{es} r_o q_o^2 g_r g_q) \end{aligned} \quad (12)$$

Similarly, the RSD of E_d is given by,

$$\begin{aligned} RSD(E_d) &= [\langle E_d^2\rangle - \langle E_d\rangle^2]/\langle E_d\rangle \\ &= [(A_{ne}^2/q_o^2 r_o^2) g_r^2 g_q^2 (g_r g_q - 1) + 2(A_{ne}A_{es} g_r/r_o)(1 - g_q) \\ &\quad + A_{es}^2 q_o^2 (g_q - 1)]^{1/2}/[(A_{ne}/r_o q_o) g_r g_q + A_{es} q_o] \end{aligned} \quad (13)$$

With no q dispersion, i.e. $g_q = 1$ and $g_r = 1 + \delta_r^2$, Eqs. (12) and (13) reduce to,

$$\begin{aligned} RSD(F_a) &= \delta_r\{1 + [2A_{ne}A_{es} r_o q_o^2 g r^2 + \\ &\quad A_{es}^2 q_o^4 r_o^2 g_r^2 (g_r^3 + g_r^2 + g_r)]/(A_{ne} + A_{es} r_o q_o^2 g_r)^2\}^{1/2} \\ &> \delta_r = RSD(r) \end{aligned} \quad (12a)$$

$$RSD(E_d) = \delta_r/(1 + A_{es} q_o^2 r_o/A_{ne} g^r) < \delta_r = RSD(r) \quad (13a)$$

Equations (12a) and (13a) are the analytical representations of the features shown in Figs. 4 and 5, namely, the widths of F_a and E_d distributions are wider and narrower, respectively, than that of the r distribution.

In the general case including the q distribution, RSD(F_a) and RSD(E_d) are numerically calculated from Eqs. (12) and (13), respectively. Some examples with the A_{ne} and A_{es} values of Eq. (3) are shown in Fig. 6. In all cases, it can be seen that the following relationship, (Eqs. 14a, b) holds well for the parameter values in the range of practical interest.

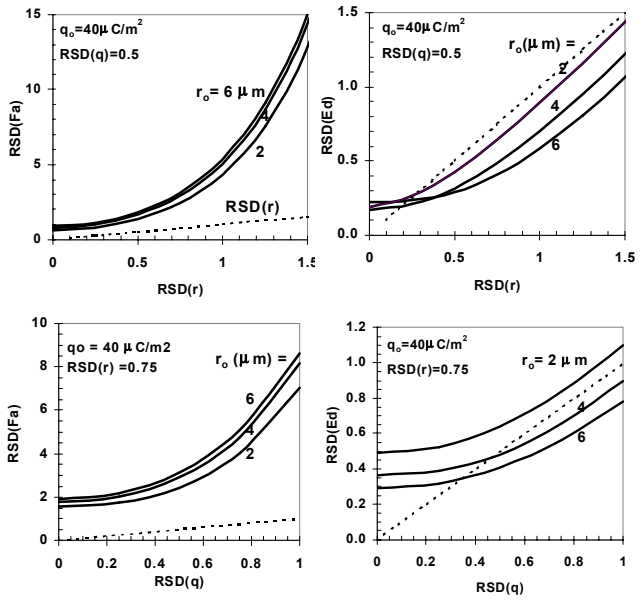

Figure 6. RSD(F_a) and RSD(E_d) from Eqs. (12 and 13), as functions of RSD(r), or RSD(q).

$$RSD(F_a) >> RSD(r) > RSD(E_d) \quad (14a)$$

$$RSD(F_a) >> RSD(q) >\approx RSD(E_d) \quad (14b)$$

Alternatively, the distributions of F_a and E_d can be studied by numerical (Monte-Carlo) simulation as follows. A random number generator is used to generate a large number N of r values that have a log-normal distribution with a median r_m and a GSD(r). Another log-normal random number generator is used to generate the same large number N of q values with a median q_m and a GSD(q). The adhesive force F_a and the detach field E_d are calculated with each set of r and q values (r_i, q_i) according to Eqs. (1) and (2), $F_{ai} = F_a(r_i, q_i)$, $E_{di} = E_d(r_i,q_i)$. Then, the CPF, P(X), where X = F_a or E_d, is determined from the number of occurrences of F_a (or E_d) in the range between 0 and X, normalized to the total number N. The PDF, p(X), can be obtained by differentiating P(X) with respect to X. The F_a (or E_d) values corresponding to P(X) = 0.16, 0.5, and 0.84, (i.e. X_1, X_m, X_2) can be interpolated from P(X), for the determination of the widths of distributions.

Examples of the F_a and E_d distributions generated with the above procedure (with N= 500,000) are shown in Figs. 7 and 8, respectively, for the case of r_m = 4μm and q_m = 40 μC/m^2, GSD(r) = 2.0 and the GSD(q) = 1.25, and the A_{es} and A_{ne} values of Eq.(3). It can be seen that the distributions are very close to log-normal. A significant difference in the widths of the F_a and E_d distributions can be seen. The median values are found at: $F_m = 0.85 \times 10^{-7}$ N and $E_m = 1.09 \times 10^7$ V/m. The X_1 and X_2 values are found to be not exactly symmetric with respect to X_m. However, generalizing the definition of GSD, we have,

$$GSD(F_a) = (F_2/F_1)^{1/2} = (2.89/0.29)^{1/2} = 3.17 \quad (19)$$

$$GSD(E_d) = (E_2/E_1)^{1/2} = (1.48/0.86)^{1/2} = 1.31 \quad (20)$$

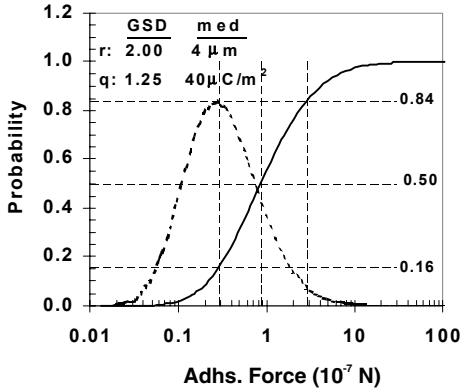

Figure 7. CPF (solid) and PDF (dashed) of adhesive force F_a, generated by Monte-Carlo simulation

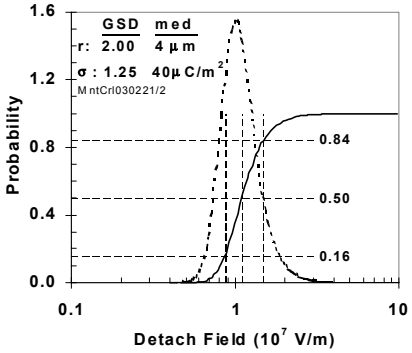

Figure 8. CPF (solid) and PDF (dashed) of detach field E_d, generated by Monte-Carlo simulation

With respect to the input GSD(r) = 2.0 and GSD(q) = 1.25, these GSD(F_a) and GSD(E_d) values satisfy the relations, Eq.(14), with RSD replaced by GSD. Such simulations have been repeated with various combinations of radius and charge density distributions as inputs. In all cases of practical interest, the relations Eq.(14) with RSD (or GSD) are confirmed.

Summary and Conclusions

In most studies of particle adhesion, the adhesive forces F_a are measured by direct comparison with mechanical forces (e.g. centrifugal or vibrational). In contrast, in electrophotography, the size of electrostatic (detach) field E_d required to remove toners from a surface is more relevant. The statistical analyses presented above show that the dispersion in F_a and E_d are generally much larger and smaller, respectively, than the dispersions in toner radius and charge density. This indicates that the dispersion,

fluctuation, or non-uniformity in the required detach field due to toner radius and charge dispersions is actually smaller than expected from measurements of mechanical adhesion forces.

References

1. D. S. Rimai, D. J. Quesnel, L. P. DeMejo, and M. T. Regan, *J. Imaging. Sci. Technol.* **45**, 179 (2001)
2. J. Hirayama, T. Nagao, O. Ebisu, H. Fukuda and I. Chen, *J. Imaging. Sci. Technol.* **47**, 9, (2003)
3. K. L. Johnson, K. Kendall and A. D. Roberts, *Proc. Roy. Soc. London*, Ser. **A324**, 301 (1971)
4. J. Atchison and A. C. Brown, *Log-Normal Distributions,* Cambridge Univ. Press, Cambridge, England, 1963
5. I. Chen, J. Appl. Phys., **45**, 4852 (1974)
6. Figure 2 of Ref. 2.

Biography

Dr. Inan Chen received his Ph.D. from the University of Michigan in 1964, and worked at Xerox Corp. in Webster, NY from 1965 to 1998. Currently, he is a consulting scientist for Quality Engineering Associates (QEA), Inc. and others, engaged in understanding the foundation physics and the characterization techniques for electrophotographic materials, processes and devices, in particular, by mathematical analysis. Contact at inanchen@aol.com